STRUCTURAL CONTROL AND HEALTH MONITORING
Struct. Control Health Monit. 2005; **12**:179–195
Published online 8 November 2004 in Wiley InterScience (www.interscience.wiley.com). DOI: 10.1002/stc.55

Seismic evaluation and innovative retrofit of a historical building in Tunisia

S. El-Borgi[1,*,†], H. Smaoui[1], F. Casciati[2], K. Jerbi[1] and F. Kanoun[1]

[1] *Applied Mechanics and Systems Research Laboratory, Tunisia Polytechnic School, B.P. 743, La Marsa 2078, Tunisia*
[2] *Department of Structural Mechanics, University of Pavia, via Ferrata 1, 27100 Pavia, Italy*

SUMMARY

This paper summarizes work conducted within the framework of a European Commission funded project on the use of appropriate modern seismic protective systems in the conservation of Mediterranean historical buildings in earthquake-prone areas. The case study is the one-and-a-half-century-old Palace of Ksar Said, located near the Capital of Tunisia. At the center of the palace, a collection of portraits and furniture are preserved in a room of great architectural and historical value which is the most precious part of the building to be protected. Ambient vibration tests were conducted to measure the acceleration at selected locations of the building. Output-only modal identification techniques were applied to extract the modal signature of the structure. A finite element model of the palace was elaborated based on the measured characteristics of stone and mortar and updated according to its measured vibratory response. Seismic vulnerability assessment of the building was carried out via three-dimensional time-history dynamic analyses of the structure. Results indicate a high vulnerability that confirms the need for intervention. A retrofit scheme is proposed that consists of a steel frame directly, attached to the portrait room structure with added fluid viscous dampers. Vulnerability assessment of the retrofitted building reveals a substantial improvement especially in the vicinity of the portrait room. Copyright © 2004 John Wiley & Sons, Ltd.

KEY WORDS: output-only modal identification; seismic vulnerability; retrofit; historical building

1. INTRODUCTION

The CHIME Project, sponsored by the European Commission, addresses the potential use of appropriate modern seismic protective systems in the preservation and conservation of Mediterranean historical buildings in earthquake-prone areas. The Tunisian case study is the Palace of Ksar Said located in a suburb of Tunis, and built in the 1850s. Great historical value is particularly attributed to the portrait room section where a valuable collection of paintings and

*Correspondence to: S. El-Borgi, Applied Mechanics and Systems Research Laboratory, Tunisia Polytechnic School, B.P. 743, La Marsa 2078, Tunisia.
†E-mail: sami.elborgi@gnet.tn

Contract/grant sponsor: European Commission
Contract/grant sponsor: Tunisia Polytechnic School

Received 3 March 2004
Revised 28 April 2004
Accepted 19 July 2004

furniture is held. Despite several repair and strengthening interventions the building has suffered severe degradation. Nevertheless, concern for preservation of the building, especially the portrait room, remains high.

The present study aims at assessing the seismic vulnerability of the Ksar Said Palace and proposing a rational retrofitting solution for protecting the portrait room. A proper seismic evaluation of the selected building requires an accurate estimation of its modal signature based on measurement of the vibratory response. Ambient vibration tests were therefore performed and the identified vibration modes were utilized to update a finite element model of the palace. Seismic vulnerability assessment of the building was then carried out via three-dimensional time-history dynamic analysis of the structure subject to a Tunis area strong motion earthquake record scaled to a peak ground acceleration specified by the seismic hazard analysis of the site. The model was used to investigate a potential retrofit system proposed to reduce the vulnerability particularly in the portrait room area.

2. DESCRIPTION OF CASE STUDY

The Tunisian case study is the Palace of Ksar Said located about 3 km north-west of the center of the capital in the Bardo district. King Sadek Bey constructed this palace in the 1850s as an additional residence for the ruling family. In the 1950s, the building was converted into a hospital until 1989, during which few minor alterations were added. Currently, it is mostly deserted except for some sections serving as administration offices or laboratories affiliated with the Tunisian Ministry of Culture. The palace with its Arab–Islamic and Italian architectural

Figure 1. View of the main facade of the case study.

styles covers an area of about 67×60 m and has three storey with different setbacks and a non-symmetric flooring system (Figures 1 and 2). The load-carrying elements consist of walls with massive stones interconnected through a weak mortar-like material. The main flooring and roofing systems consist of brick vaults with an earth filling standing on the wall, with or without steel joists. Repairs and strengthenings made at different periods of time introduced a variety of construction systems, including reinforced concrete slabs.

At the center of the palace is the portrait room, home to a unique collection of 18th and 19th century paintings, standing out with its all-marble floor and columns. The motivation for preservation of the portrait room stems from its historical and cultural value, but is also justified by the apparent weakness of the structural system around it (Figure 3). Along the four sides of

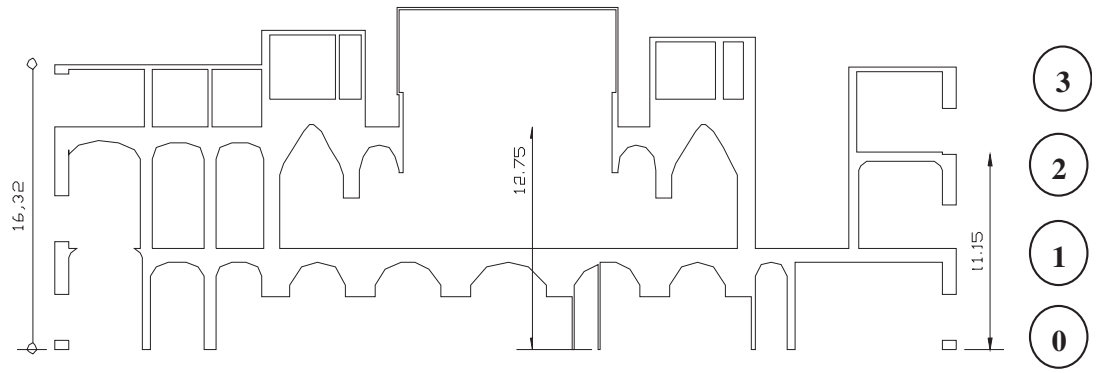

Figure 2. Typical cross-section of the case study (dimensions in meters).

Figure 3. View of the portrait room.

the room extends a gallery with the top resting on four lines of columns. The brittle marble columns support the vaulted roof and are supported in turn by the floor structure underneath. Moreover, the poor design of the joints at the ends of these columns should not be overlooked.

3. SEISMIC EVALUATION OF EXISTING BUILDING

3.1. Methodology

A proper seismic evaluation of the selected building requires accurate estimation of its modal signature (i.e. frequencies, mode shapes and damping ratios) based on measurement of the vibratory response. Ambient vibration tests were therefore performed to measure the acceleration at selected locations of the building. Output-only modal identification techniques were applied to extract the modal signature of the building. A finite element model of the palace was developed and updated, based on the measured characteristics of stone and mortar and the first two measured natural periods. Seismic vulnerability assessment of the building was carried out via three-dimensional time-history dynamic analysis of the structure subject to a Tunis area strong motion earthquake record scaled to a peak ground acceleration specified by the seismic hazard analysis of the site.

3.2. Material characterization

A series of experimental tests were conducted to determine the mechanical properties of stone and mortar samples extracted from debris of the monument. Owing to the preservation regulations, sample extraction from most parts of the building, especially the better-preserved interior, was not permitted. As a result, all the samples used were taken from damaged parts of external walls. Naturally, this induces a bias, with data based on rather altered material, and relevant to only a selected part of the building. Moreover, test results exhibited large scatter which reflects pronounced heterogeneity in the characteristics of the materials and made it difficult to suggest a significant representative estimate.

Based on compression tests and flexural tensile tests on stone specimen, block compressive and tensile average strengths were evaluated at $f_{bc} = 18$ MPa and $f_{bt} = 4.9$ MPa, respectively. For mortar, compressive and flexural tensile average strengths were estimated at $f_{mc} = 2.7$ MPa and $f_{mt} = 0.42$ MPa, respectively. Equivalent properties for masonry are determined, based on available empirical rules [1]. A key parameter is the compressive strength f_{wc} which is estimated at 4.50 MPa, based on values given by several alternative formulae, ranging between 2 and 6 MPa. The modulus of elasticity is given by $E_{wc} = 1000\, f_{wc} = 4500$ MPa [1]. Poisson's ratio is taken as $v = 0.16$. Finally, the tensile strength of the masonry is estimated at $f_{wt} = 2/3\, f_{mt} = 0.28$ MPa.

The compressive strength of concrete forming the floor slabs is measured experimentally by a nondestructive technique. Results indicate a compressive strength $f_{cc} = 8.7$ MPa. The tensile strength is deduced as $f_{ct} = 0.06\, f_{cc} + 0.6 = 1.12$ MPa.

3.3. Ambient vibration testing

For large structures, ambient vibration tests with output-only measurements are preferred over forced vibration tests where both the excitation and the response are measured [2–3]. In ambient

vibration testing, the measured response is representative of the actual operating conditions of the structure which vibrates under its natural excitation loads such as wind, micro-tremors, traffic and human activity.

3.3.1. Description of the ambient vibration measurement equipment. Ambient vibration tests were conducted on the case study using a 16-channel data acquisition system, called Vibration Survey System, Model VSS-3000 [4], with nine force-balance uniaxial accelerometers, model FBA-ES-U [5]. A picture of the data acquisition and measurement equipment is shown in Figure 4.

The sensors, which are set to measure an acceleration range of $\pm 0.25g$ with a resolution of $0.1\,\mu g$, convert the physical excitation into electrical signals. Each accelerometer is connected to the data acquisition system using a 100-m-long cable. Cables are used to transmit the electronic signals from sensors to the signal conditioner. A signal conditioner unit is used to improve the quality of the signals by removing undesired frequency contents (filtering) and amplifying the signals.

The amplified and filtered analog signals are converted to digital data using a 16-bit resolution analog-to-digital converter at a speed of 1000 kHz prior to storage on the data acquisition computer. The analog-to-digital converter is controlled by a data acquisition computer using a custom program called DasyLab, version 5.6, by National Instruments. The analog-to-digital converter is capable of sampling up to 16 channels at sampling frequencies between 0.2 Hz to 2000 Hz. Vibration experiments were conducted during 10 minutes at a sampling frequency of 100 Hz with all channels set for a low-pass filter of 40 Hz. Signals converted to digital form are stored on the hard disk of the data acquisition computer in ASCII form.

3.3.2. Planning of the test set-ups. The sensors were placed at selected locations of the building levels to measure the horizontal components of the acceleration at each point. Four accelerometers were utilized as reference sensors at two points on the roof level and the remaining sensors were used as roving sensors. A total of 30 set-ups were accomplished to provide sufficient data for accurate identification of the modal signature. A preliminary dynamic analysis of the structure was performed using a three-dimensional finite element model in order

Figure 4. Picture of the data acquisition system and measurement equipment.

to help plan the set-ups and determine judicious locations for the accelerometers which included a total of 72 points.

3.4. Output-only modal identification

The complex non-stationary nature of the unmeasured excitation requires the use of robust output-only modal identification techniques which include the frequency domain decomposition [6] and the stochastic subspace identification methods [7]. These methods have recently been applied successfully to buildings and bridges [8–9].

In the present study, the frequency domain decomposition (FDD) method and two stochastic subspace identification methods, namely the unweighted principal component algorithm (SSI-UPC) and the canonical variate analysis algorithm (SSI-CVA), were applied to extract the modal signature of the historic building using the computer program Artemis Extractor [10]. The FDD technique provides estimates of only the identified natural periods and mode shapes whereas the SSI-UPC and the SSI-CVA algorithms provide estimates of the entire modal signature. Figure 5 shows the average of normalized singular values of spectral density matrices of all data sets, using the FDD technique. The singular values in this plot correspond to the detected frequencies.

Table I shows the measurement-based estimates of the natural periods of the first five modes using FDD, SSI-UPC and SSI-CVA techniques which are in very close agreement. On the other hand, the damping ratios estimated by the SSI-UPC and SSI-CVA techniques show a relative variability and range approximately in the interval between 2% and 6%. Figure 6 shows the measurement-based mode shapes identified using the FDD technique.

3.5. Finite element modeling

A three-dimensional finite element model of the building was elaborated with the SAP2000 computer program [11] based on a detailed geometric model. The model, shown in Figure 7,

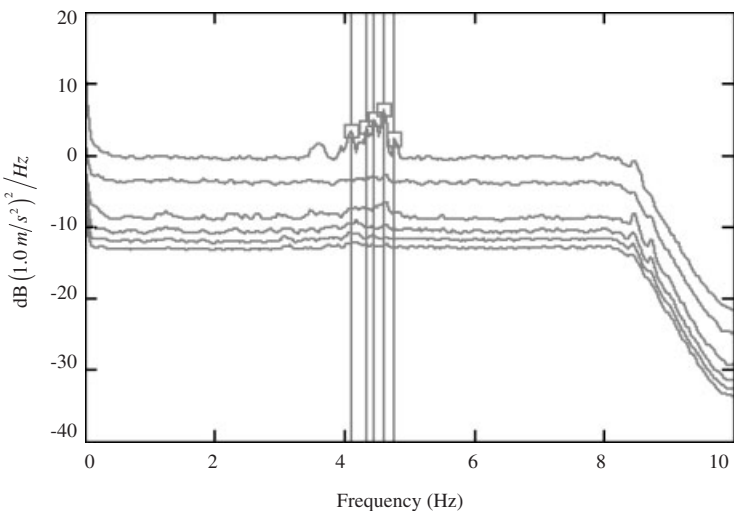

Figure 5. Average of normalized singular values of spectral density matrices of all data sets using FDD algorithm.

Table I. Measurement-based natural periods and damping ratios for various identification techniques.

	Estimated from measurements					
	FDD		SSI-UPC		SSI-CVA	
Mode	Natural period (s)	Damping ratio (%)	Natural period (s)	Damping ratio (%)	Natural period (s)	Damping ratio (%)
1	0.243	—	0.236	4.79	0.233	3.05
2	0.231	—	0.231	4.75	0.232	2.46
3	0.225	—	0.224	3.70	0.224	2.56
4	0.217	—	0.221	4.67	0.221	5.36
5	0.210	—	0.219	2.38	0.219	5.89

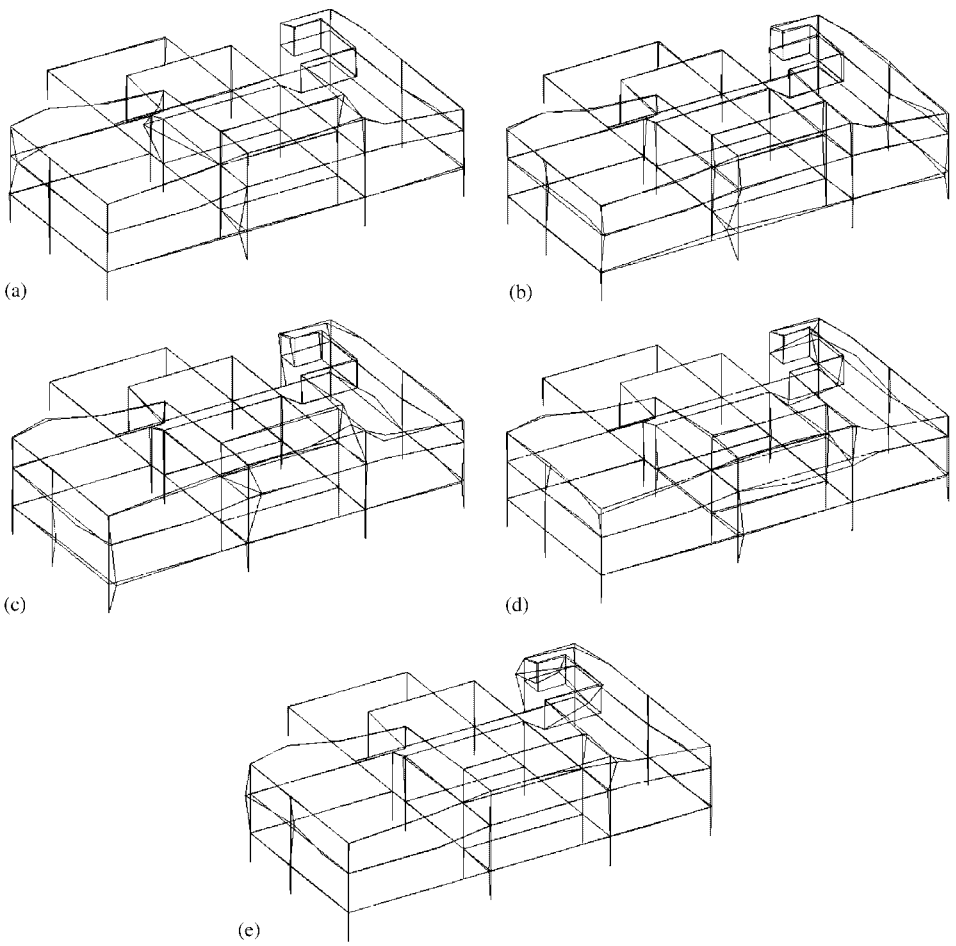

Figure 6. First five modes of vibration identified using the FDD technique. (a) First mode shape; (b) Second mode shape; (c) Third mode shape; (d) Fourth mode shape and (e) Fifth mode shape.

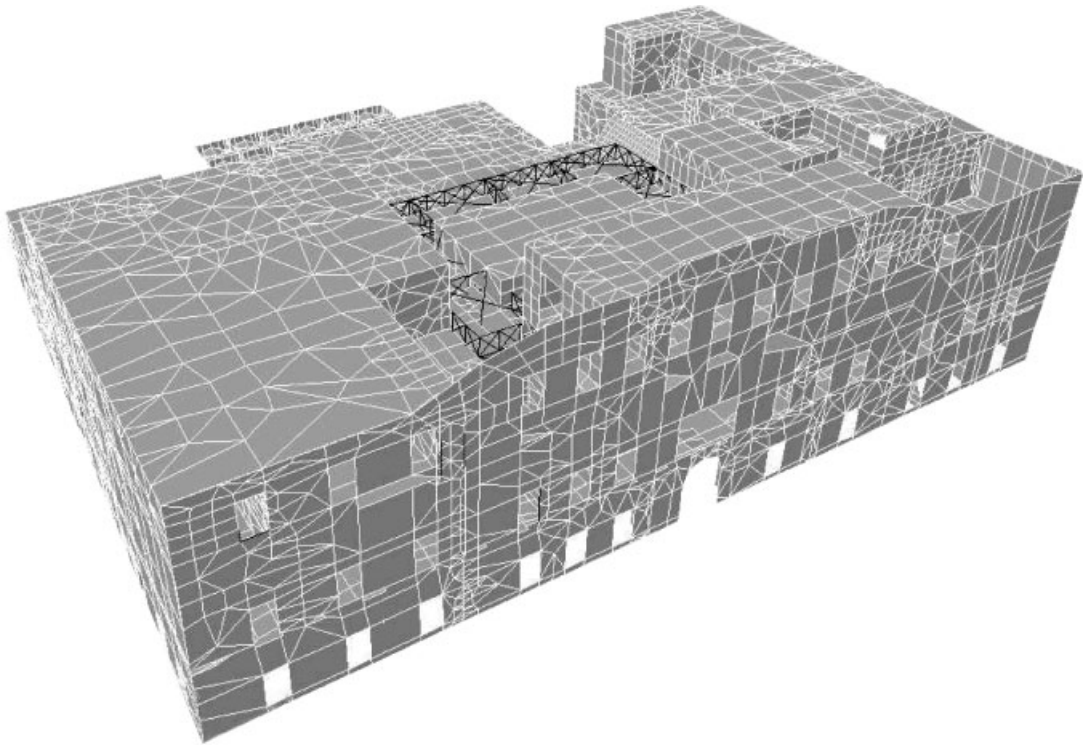

Figure 7. Finite element model of the palace.

Table II. Computed natural periods before and after updating.

Mode	Natural period before updating (s)	Natural period after updating (s)
1	0.397	0.249
2	0.360	0.218
3	0.317	0.190
4	0.265	0.155
5	0.242	0.145

uses a total of 17919 shell and beam elements. The material behavior is assumed to be linear elastic, isotropic and homogeneous.

The real behavior actually does not obey these assumptions. The masonry is essentially nonhomogeneous and anisotropic at the macroscopic scale with different mechanical characteristics along directions parallel and normal to bed joints, and the behavior is no longer linear elastic near failure. Nevertheless, the adopted simplified behavior remains a meaningful approximation for the purpose of vulnerability analysis.

The preliminary finite element model was based on estimates of the material properties reported in Section 3.2 and which bear a significant degree of uncertainty, given the underlying scatter in test data. Finite element calculation of the modal signature using these characteristics for all masonry elements yields the fundamental periods shown in Table II. The computed fundamental period $T_1 = 0.397$ s is 63% away from the measured period identified by the FDD technique. This clearly indicates the need for model updating.

The measured fundamental period can be approached simply by scaling up the Young's modulus uniformly for the entire building. However, the difference in material quality of internal and external elements would be ignored. A preferred approach is to consider separate moduli for internal and external walls in order to reflect the apparent difference in material properties. The two conditions chosen for determining the two unknowns consist in matching the experimental and calculated values for the first two periods T_1 and T_2. Advantage is taken of the fact that the natural period is inversely proportional to the square root of Young's modulus. This makes it easy to target a point (E'_e, E'_i), with a prescribed period T', on the proportional line from a point (E_e, E_i) with a known period T. Therefore, it can be written:

$$(E'_e, E'_i) = (\alpha E_e, \alpha E_i) \quad \text{with} \quad \alpha = (T/T')^2$$

The updating was based on the measured periods identified by the FDD technique. An approximate search provided the values $E_{we} = 4500$ MPa and $E_{wi} = 12500$ MPa for external and internal walls respectively. The last column of Table II reports the computed periods after updating. The updated calculated periods are $T_1 = 0.249$ s and $T_2 = 0.218$ s which are respectively 2.5% and -5.1% away from the experimental values identified by the FDD technique. After correcting the finite element model, the compressive and tensile strength of the walls were adjusted, based on the location of the wall whether interior or exterior. The exterior wall compressive strength is $f_{wce} = 4.50$ MPa and that of the interior wall is $f_{wci} = 12.5$ MPa. The exterior wall tensile strength is $f_{wte} = 0.28$ MPa and that of the interior wall is $f_{wti} = 0.77$ MPa.

3.6. Seismic vulnerability analysis

Geotechnical investigations near the building site showed that the soil has a low compressibility with a relatively high strength and is mostly stiff clay with sand or gravel lenses [12]. A recent seismic hazard analysis of the Grand Tunis area indicates that the peak ground acceleration (PGA) is $0.22g$ for a 500-year return period earthquake [12]. The latest earthquake that caused damage in the Grand Tunis area and specifically in the Bardo district occurred in December 1970 with a magnitude of 5.1 on the Richter scale.

Seismic vulnerability assessment of the building was carried out via three-dimensional time response dynamic analysis of the structure subject to a Tunis area strong motion earthquake record: the Ezzahra Earthquake which occurred on 24 April 2000. The North–South component of the earthquake is utilized and the magnitude of the peak ground acceleration (PGA) is scaled up to the peak values of $0.22g$ for a relatively strong earthquake (Figure 8) and $0.10g$ for a moderate earthquake. The record has a duration of 16.63 s with a sampling frequency of 0.005 s.

For each value of the PGA, dynamic stresses are computed under a combination of dead load, service loads and earthquake excitations. Moreover, four configurations of earthquake actions are considered for each loading combination. The first consists of the full earthquake

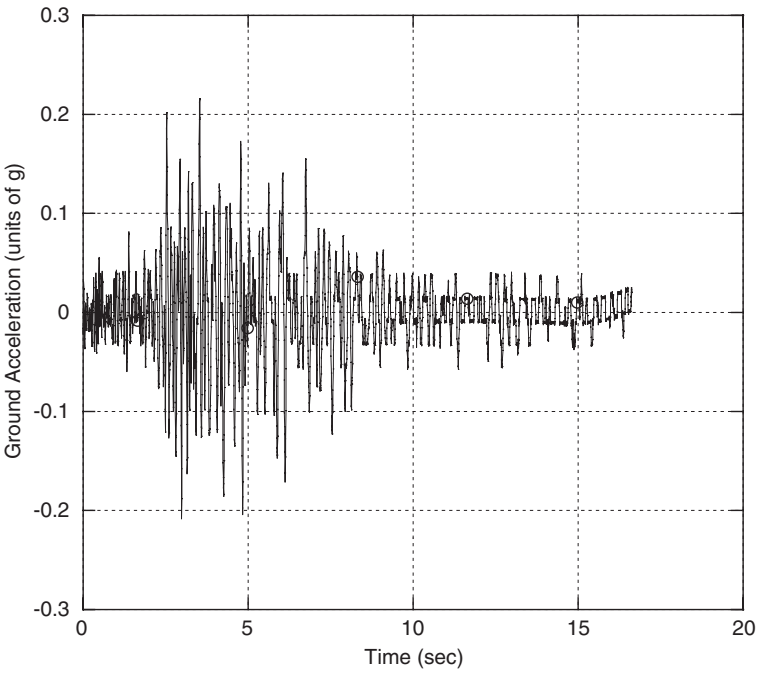

Figure 8. Ezzahra (suburb of Tunis) earthquake, 24 April 2000, NS component, scaled to a peak ground acceleration of $0.22g$.

acting along one reference direction and a 30% fraction of the same earthquake acting on a perpendicular direction. The second configuration is defined in a similar way, except that the weaker earthquake is applied in the opposite direction. The two other configurations are defined by rotating the first two by 90°.

For failure analysis a masonry-specific plane failure criterion is adopted [1]. The failure line is made up of a von Mises criterion for states of biaxial compression (BC). For states of biaxial tension (BT) and biaxial tension–compression (BTC) the line is completed by linear interpolation from failure states of pure tension and pure compression. A further approximation is made by assuming the same biaxial failure criterion when the shearing stress is non-vanishing. The failure function, shown schematically in Figure 9, for the exterior and interior masonry wall can be expressed piecewise as follows:

$$F_1(\sigma) = J_2^{1/2} - f_{\mathrm{wc}}$$
$$F_2(\sigma) = \sigma_2 + \sigma_1 - f_{\mathrm{wt}}$$
$$F_3(\sigma) = -\sigma_1 + \sigma_2 f_{\mathrm{wc}}/f_{\mathrm{wt}} - f_{\mathrm{wc}}$$
$$F_4(\sigma) = \sigma_1 - \sigma_2 f_{\mathrm{wt}}/f_{\mathrm{wc}} - f_{\mathrm{wt}}$$

where J_2 is the second invariant of the deviatoric stress tensor and σ_1 and σ_2 are the principal stresses.

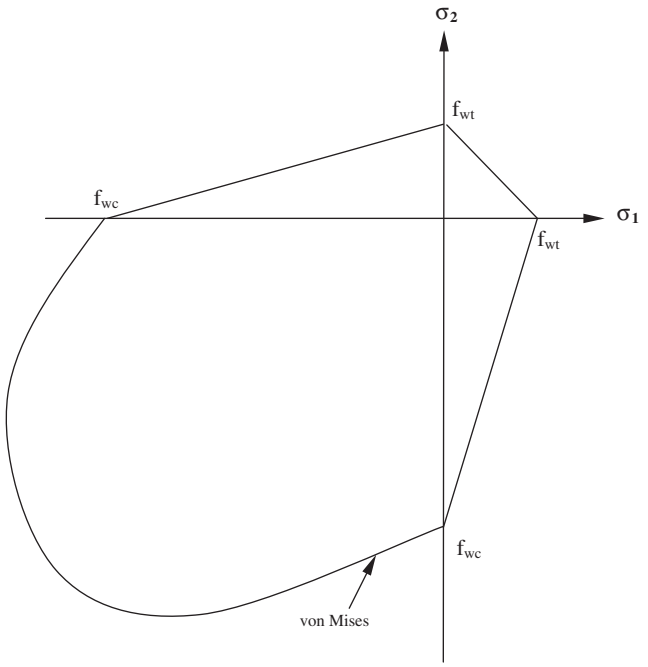

Figure 9. Masonry failure criterion.

Table III. Vulnerability analysis results of the existing palace.

	Total number of nodes	Number of nodes where failure occurred		Percentage (%)	
		PGA 0.22*g*	PGA 0.10*g*	PGA 0.22*g*	PGA 0.10*g*
Whole structure	16932	14164	8420	83.7	49.7
Biaxial tension–compression (BTC)		12202	5659	72.1	33.4
Biaxial tension (BT)		10155	6276	60.0	37.1
Biaxial compression (BC)		40	3	0.24	0.02

Damage is evaluated according to the adopted masonry failure criterion by considering at each joint the envelope of the yield function over the complete set of loading cases. The ratio of number of damaged spots to the total number of points is taken as a measure of seismic vulnerability. Statistics of damage in the building as a whole are summarized in Table III. Overall vulnerability of the palace subjected to a 0.22*g* earthquake is estimated at 83.7%, with biaxial tension–compression as the predominant type of failure (72.1%), followed by biaxial tension (60%) and only 0.24% for biaxial compression. Analysis of the building in the case of a PGA of 0.1*g* reveals a vulnerability of 49.7%. Hence, the model indicates that the level of damage remains high, even under a moderate earthquake of 0.1*g*. According to the calculated seismic vulnerability, the Ksar Said Palace clearly is in need of protection against earthquake

Table IV. Vulnerability of the portrait room without retrofit.

	Total number of nodes	Number of nodes where failure occurred		Percentage (%)	
		PGA 0.22*g*	PGA 0.10*g*	PGA 0.22*g*	PGA 0.10*g*
Portrait room	1843	1731	1205	93.9	65.4
Biaxial tension–compression (BTC)		1430	768	77.6	41.7
Biaxial tension (BT)		1325	907	71.9	49.2
Biaxial compression (BC)		10	0	0.54	0.0

hazard. Focusing on the portrait room zone, the statistics indicate higher than average vulnerabilities, as reported in Table IV, which shows likelihood of total damage under a 0.22*g* earthquake.

4. VULNERABILITY ASSESSMENT OF RETROFITTED BUILDING

The outstanding character and value of the portrait room as well as its extreme vulnerability suggest that, under budget restraints, priority be given to a localized retrofit.

4.1. Proposed retrofit solution

The proposed retrofit scheme consists of a steel frame (Figure 10) to be erected around the portrait room from the ground floor up to the roof level and be adequately fixed to the walls and floors in order to allow transfer of vertical and horizontal forces to the steel structure. The framing elements are dissimulated within the existing masonry whenever possible, otherwise thin walls are added to preserve the architectural aspect of the building. In addition to the steel structure, damping is introduced by installing diagonally the fluid viscous dampers shown in Figure 11. These are linear viscous dampers which develop forces given by $\boldsymbol{F} = c\boldsymbol{v}$, where $\boldsymbol{v}$ denotes the rate of relative displacement of the damper ends and c is the damping coefficient of the damper. The retained damping coefficients are $c_1 = 40\,\mathrm{MNs/m}$ for the top-level dampers and $c_2 = 70\,\mathrm{MNs/m}$ for those located at the first and second floors.

4.2. Vulnerability analysis and discussion of results

In order to assess the gain achieved by the retrofit solutions, vulnerability analysis is performed on the retrofitted palace. First, the steel frame is considered alone to assess the sole effect of structure stiffening. Then, dampers are included and the gain achieved by the complete retrofit system is determined.

The results for the first scenario are given in Tables V and VI. For the palace as a whole the gain, measured by arithmetic improvement in vulnerability, is 12.4% for the PGA of 0.22*g* and 14.5% for 0.1*g*. For the portrait room the gain is remarkably higher for both peak ground accelerations : 20.1% and 28.5% respectively.

With damping added, the gain is improved to 18.7% for 0.22*g* PGA earthquake (21.1% for 0.1*g* PGA earthquake) for the entire palace (Table VII). For the portrait room the gain improved to 26.8% for 0.22*g* PGA earthquake (37.2% for 0.1*g* PGA earthquake, Table VIII).

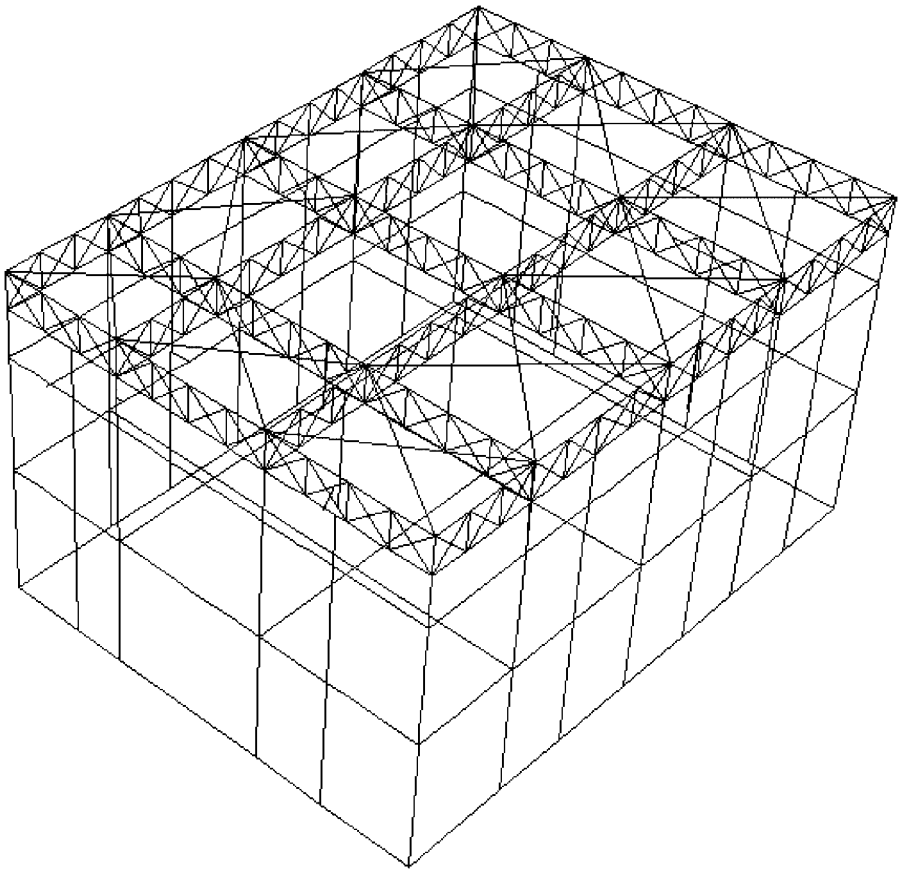

Figure 10. Portrait room retrofit steel frame system.

Under the 0.22*g* PGA earthquake the maximum force in the dampers was estimated at 42 t at the top level, 263 t at the second and 293 t at the lowest level.

Thus, the vulnerability results show a definite and substantial reduction in damage level, and clearly demonstrate the capability and potential of the proposed retrofit technique, although the vulnerability has not been improved to a satisfactory level. Indeed, these gains are obtained by a retrofit system confined to only a small part of the building and it is expected that a similar retrofit system that is extended to a lager portion of the structure would be capable of bringing vulnerability down to the desired level.

5. CONCLUSIONS

This paper summarizes work conducted within the framework of a European Commission funded project on the use of appropriate modern seismic protective systems in the conservation

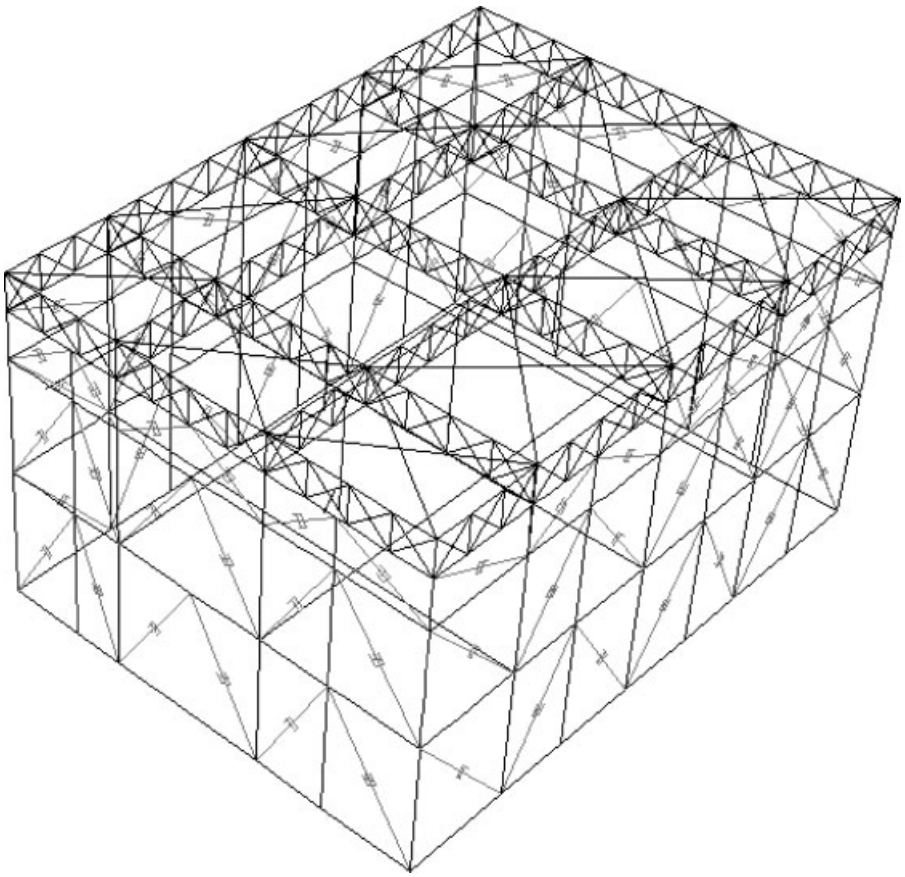

Figure 11. Retrofit steel frame–damper system.

Table V. Vulnerability of the palace after retrofit by steel frame alone.

	Total number of nodes	Number of nodes where failure occurred		Percentage (%)	
		PGA 0.22*g*	PGA 0.10*g*	PGA 0.22*g*	PGA 0.10*g*
Whole structure	17358	12370	6105	71.3	35.2
Biaxial tension–compression (BTC)		9635	3671	55.5	21.2
Biaxial tension (BT)		8796	4519	50.7	26.0
Biaxial compression (BC)		55	8	0.32	0.05

of Mediterranean historical buildings in earthquake-prone areas. The case study is the one-and-a-half-century-old Palace of Ksar Said, located near the Capital of Tunisia.

Ambient vibration tests were performed on the palace and a series of experimental tests were conducted to determine the mechanical properties of stone and mortar samples extracted from

Table VI. Vulnerability of the portrait room after retrofit by steel frame alone.

	Total number of nodes	Number of nodes where failure occurred		Percentage (%)	
		PGA 0.22*g*	PGA 0.10*g*	PGA 0.22*g*	PGA 0.10*g*
Portrait room	2024	1493	747	73.8	36.9
Biaxial tension–compression (BTC)		1135	480	56.1	23.7
Biaxial tension (BT)		1050	490	51.9	24.2
Biaxial compression (BC)		0	0	0.0	0.0

Table VII. Vulnerability of the palace after retrofit by steel frame–damper system.

	Total number of nodes	Number of nodes where failure occurred		Percentage (%)	
		PGA 0.22*g*	PGA 0.10*g*	PGA 0.22*g*	PGA 0.10*g*
Whole structure	17531	11390	5014	65.0	28.6
Biaxial tension–compression (BTC)		8679	2812	49.5	16.0
Biaxial tension (BT)		7844	3717	44.7	21.2
Biaxial compression (BC)		47	8	0.27	0.05

Table VIII. Vulnerability of the portrait room after retrofit by steel frame–damper system.

	Total number of nodes	Number of nodes where failure occurred		Percentage (%)	
		PGA 0.22*g*	PGA 0.10*g*	PGA 0.22*g*	PGA 0.10*g*
Portrait room	2079	1394	586	67.1	28.2
Biaxial tension–compression (BTC)		1048	312	50.4	15.0
Biaxial tension (BT)		923	383	44.4	18.4
Biaxial compression (BC)		0	0	0.0	0.0

debris of the monument. The complex non-stationary nature of the unmeasured excitation, due essentially to wind, traffic, micro-tremors and human activity, requires the use of output-only modal identification techniques that must be robust with respect to this non-stationarity. Two such methods, namely the frequency domain decomposition (FDD) and the stochastic subspace identification techniques (SSI), were applied to extract the modal signature of the studied historic building. The measurement-based estimates of the natural periods of the first five modes using the FDD and SSI techniques were found to be in very close agreement. On the other hand, the damping ratios estimated by the SSI techniques showed a relative variability and ranged in the interval between 2% and 6%.

A preliminary finite element model was elaborated based on estimates of the material properties of stone and mortar samples extracted from debris of the monument, which bear a

significant degree of uncertainty. Finite element calculation of the modal signature using these characteristics yielded a fundamental period that is 63% away from the measured period identified by the FDD technique, which clearly indicates the need for model updating. The updating approach consisted of considering separate elastic moduli for internal and external walls in order to reflect the apparent difference in material properties. The two conditions chosen for determining the two unknowns consisted in matching the experimental (FDD) and calculated values for the first two periods T_1 and T_2. Advantage is taken of the fact that the natural period is inversely proportional to the square root of Young's modulus. The updating was based on the measured periods identified by the FDD technique. An approximate search provided the values of the modulus of elasticity for external and internal walls. The updated calculated periods are $T_1 = 0.249$ s and $T_2 = 0.218$ s which are respectively 2.5% and -5.1% away from the experimental values identified by the FDD technique.

With a calibrated model of the building, seismic vulnerability assessment was carried out via three-dimensional time response dynamic analysis of the structure subject to a Tunis area strong motion earthquake record. The seismic excitation was scaled to a PGA of $0.22g$ and $0.10g$ representing, respectively, relatively strong and moderate earthquakes. Dynamic stresses were computed and damage was evaluated according to a masonry-specific plane failure criterion. The estimated damage statistics indicate that the existing building is quite vulnerable and in particular the portrait room.

A strengthening scheme was proposed to retrofit the portrait room with a steel frame to be erected around it from the ground floor up to the roof level. A number of fluid viscous dampers were added diagonally to the steel frame in order to enhance the damping performance of the structure. The vulnerability results show a definite and substantial reduction in damage level, and clearly demonstrate the capability and potential of the proposed retrofit technique.

ACKNOWLEDGEMENT

The authors are grateful for the funding provided by the European Commission and Tunisia Polytechnic School. Sincere thanks are due to the technical personnel who assisted the authors in conducting the ambient vibration tests on the palace.

REFERENCES

1. Syrmakezis CA, Chronopoulos MP, Sophocleous AA, Asteris PG. Structural analysis methodology for historical buildings. *Architectural Studies*, *Materials and Analysis*, Brebbia CA, Leftheris B (eds), WIT Press, 1995; 373–382.
2. Brincker R, Anderson P. A way of getting scaled mode shapes in output only modal testing. *Proceedings of the 21st International Modal Analysis Conference*, Kissimmee, Florida, USA, February 2003.
3. Brincker R, Ventura C, Anderson P. Why output-only modal testing is a desirable tool for a wide range of practical applications. *Proceedings of the 21st International Modal Analysis Conference*, Kissimmee, Florida, USA, February 2003.
4. Kinemetrics Inc. *Operating Instructions for Vibration Survey System*, *Model VSS-3000*, 1997.
5. Kinemetrics Inc. *User's Guide for the EpiSensor Force Balance Accelerometers*, *Model FBA ES-U*, 2000.
6. Brincker R, Andersen P. Ambient response analysis of the Heritage Court Building structure. *Proceedings of the 18th International Modal Analysis Conference* (*IMAC*), San Antonio, Texas, 2000; 1081–1087.

7. Van Overschee P, De Moor B. *Subspace Identification for Linear Systems*: *Theory*, *Implementations and Applications*. Kluwer: Dordrecht, 1996.
8. Brincker R, Andersen P, Zhang L. Modal identification from ambient responses using frequency domain decomposition. *Proceedings of the 18th International Modal Analysis Conference* (*IMAC*), San Antonio, Texas, 2000; 625–630.
9. Brincker R, Andersen P, Frandsen JB. Ambient response analysis of the Great Belt Bridge. *Proceedings of the 18th International Modal Analysis Conference* (*IMAC*), San Antonio, Texas, 2000; 26–32.
10. Artemis Extractor Program Overview. http://www.svibs.com, accessed 15 February 2004.
11. Computers and Structures Inc. *SAP2000*: *Three Dimensional Static and Dynamic Finite Element Analysis and Design of Structures*, 2000.
12. Kacem J, Dlala M, Mejri L, Ben Abdallah S, Dhouibi R, Oueslati F. Seismic hazard analysis of Tunisia. *Report D2 to the European Commission. CHIME project* (Conservation of Historical Mediterranean Sites by Innovative Seismic Techniques). Marcellini A, Syrmakezis C (eds). November 2001.

